

Collisionless loss-cone refilling: there is no final parsec problem

Alessia Gualandris^{1*}, Justin I. Read¹, Walter Dehnen² and Elisa Bortolas³

¹*Department of Physics, Faculty of Engineering and Physical Sciences, University of Surrey, Guildford, GU2 7XH, United Kingdom*

²*Department of Physics and Astronomy, University of Leicester, Leicester, LE1 7RH, United Kingdom*

³*INAF-Osservatorio Astronomico di Padova, Vicolo dell'Osservatorio 5, I-35122, Padova, Italy*

ABSTRACT

Coalescing massive black hole binaries, formed during galaxy mergers, are expected to be a primary source of low frequency gravitational waves. Yet in isolated gas-free spherical stellar systems, the hardening of the binary stalls at parsec-scale separations owing to the inefficiency of relaxation-driven loss-cone refilling. Repopulation via collisionless orbit diffusion in triaxial systems is more efficient, but published simulation results are contradictory. While sustained hardening has been reported in simulations of galaxy mergers with $N \sim 10^6$ stars and in early simulations of rotating models, in isolated non-rotating triaxial models the hardening rate continues to fall with increasing N , a signature of spurious two-body relaxation.

We present a novel approach for studying loss cone repopulation in galactic nuclei. Since loss cone repopulation in triaxial systems owes to orbit diffusion, it is a purely collisionless phenomenon and can be studied with an approximated force calculation technique, provided the force errors are well behaved and sufficiently small. We achieve this using an accurate fast multipole method and define a proxy for the hardening rate that depends only on stellar angular momenta. We find that the loss cone is efficiently replenished even in very mildly triaxial models (with axis ratios 1 : 0.9 : 0.8). Such triaxiality is unavoidable following galactic mergers and can drive binaries into the gravitational wave regime. We conclude that there is no ‘final parsec problem’.

Key words: (galaxies:) quasars: supermassive black holes – gravitational waves – stars: kinematics and dynamics – methods: numerical

1 INTRODUCTION

Supermassive black hole binaries (BHBs) are expected to form efficiently through cosmic time as a result of galaxy mergers, if the original galaxies contain a central massive black hole (MBH) (Begelman et al. 1980). In the early stages of the merger, the MBHs are dragged towards each other by dynamical friction, until they form a binary system. The binary continues to evolve and harden by gravitational interactions with stars that come within a few binary separations. As a result of such encounters, stars subtract energy and angular momentum from the binary, and they are ejected to larger distances. N -body simulations of galaxy mergers (e.g. Quinlan & Hernquist 1997; Milosavljević & Merritt 2001; Gualandris & Merritt 2012) show a decrease in the central stellar density and the formation of a core. This process, often called *core scouring*, may be responsible for the observation of cores in massive elliptical galaxies (Lauer

1985; Lauer et al. 1995; Faber et al. 1997; Graham 2004; Lauer et al. 2005; Ferrarese et al. 2006; Graham 2013). If a sufficient supply of stars is available in the merger remnant to interact with the binary, hardening continues down to separations where emission of gravitational waves becomes important. The evolution then proceeds rapidly to inspiral and black hole coalescence. The recent detections of gravitational wave signals (GW150914 and GW151226) by Advanced Ligo (Abbott et al. 2016a,b) from the merger of two stellar mass black holes proves very strongly that black holes exist, they form binaries, and merge within a Hubble time due to emission of gravitational waves. The same is expected for MBHs, and several missions and detectors are being planned in the hope to detect gravitational waves from BHBs. In the context of BHBs, The Pulsar Timing Array (PTA) (e.g. Babak et al. 2016), which is already operational, is the most suitable to detect gravitational waves from the most massive BHBs, while the eLISA space-based interferometer (Barausse et al. 2015) will be sensitive to the frequencies typical of lower mass BHBs, like the Milky Way’s

* E-mail: a.gualandris@surrey.ac.uk

MBH. Detection of BHBs in the gravitational waves window would provide crucial information on the masses, spins, orientations and even distances of the two black holes. It would also provide an exciting new cosmological probe, given that BHBs can in principle be seen right back to the beginning of the Universe (Hogan et al. 2009).

All efforts to detect gravitational waves from BHBs are based on the assumption that the binaries do in fact coalesce efficiently, i.e. a significant fraction have a timescale for emission of gravitational radiation shorter than a Hubble time. This assumption seems to be corroborated by observations: despite strong efforts to detect BHBs with a variety of techniques, only a handful of candidates exist, and for most of these systems alternative explanations have been put forward (for a review see e.g. Dotti et al. 2012). It appears that BHBs find a way to coalescence, but the mechanism for this remains to be understood. While gas may play a role in bringing BHBs into the gravitational wave regime, there is evidence for little or no gas in massive elliptical galaxies, and works by Cuadra et al. (2009) and Lodato et al. (2009) show that gas discs are only efficient at driving mergers of BHBs for low mass MBHs. This suggests that if BHBs merge, in many cases they must do so in the absence of gas. In this paper, we consider only pure stellar systems devoid of gas.

Theoretically, the ultimate fate of BHBs depends on the supply of stars to the binary’s loss cone, i.e. the region in phase space characterised by low enough angular momentum to ensure interaction with the binary. If the reservoir of stars on intersecting orbits is depleted and the loss cone cannot be maintained sufficiently populated, the binary’s evolution will dramatically slow down or even stall (Begelman et al. 1980).

There are two distinct classes of physical mechanisms for loss cone refilling in the absence of gas: collisional processes and collisionless processes. In idealised spherical galaxies, the evolution of BHBs slows down after all stars initially on loss cone orbits are ejected, which occurs on a dynamical timescale. Repopulation of the loss cone in such models is due solely to two body relaxation, i.e. a collisional process. This operates on the relaxation timescale, which for most galaxies is much longer than the Hubble time, and implies that the binary is in the empty loss cone regime at all times (Milosavljević & Merritt 2001, 2003). In N -body simulations of isolated spherical models, this regime can be identified by the N -dependence of the binary hardening rate, since the relaxation time scales approximately as $N/\log N$ (Makino & Funato 2004; Berczik et al. 2005; Merritt et al. 2007). The earliest simulations, however, did not observe this scaling due to the low N used which implied a very short relaxation time and therefore a full loss cone (e.g. Milosavljević & Merritt 2001). Collisional processes are rather inefficient at repopulating the loss cone in real galaxies, and are not sufficient to lead BHBs to coalescence in a Hubble time. However, they need to be treated very carefully since they introduce a spurious population of loss cone orbits in any N -body simulation where N is smaller than the true number of stars.

In non-spherical galaxies, refilling of the loss cone can proceed due to collisionless “diffusion” in angular momentum. Torques from a non-spherical potential cause stellar angular momenta to change on a timescale which is much shorter than the relaxation time, though typically longer

than radial orbital periods (Merritt 2013; Pontzen et al. 2015). In axisymmetric nuclei, stellar orbits conserve only energy and the component J_z of angular momentum parallel to the symmetry axis. While the total angular momentum J is not conserved, conservation of J_z implies that there is a lower limit to how small J can become due to diffusion. In this sense, orbits in axisymmetric potentials are not truly centrophilic, but they reach very small radii and contribute to loss cone refilling. There are two families of orbits in flattened potentials: the tube orbits, regular orbits for which J is approximately conserved, and saucer orbits, for which J can become very small. The fraction of stars on saucer orbits depends on the degree of flattening in the system. In triaxial nuclei, J is not conserved and truly centrophilic orbits are possible. In addition to two families of tube orbits and saucer orbits, there exists a new family of orbits, called pyramids, which can achieve arbitrarily low values of J (Merritt & Vasiliev 2011). All stars on pyramid orbits eventually reach the centre, though the timescale can vary. While the fraction of saucer orbits in axisymmetric models is expected to be small, the fraction of pyramid orbits in triaxial models can be very high (Poon & Merritt 2004). This suggests that collisionless loss cone refilling may be efficient at driving BHBs to coalescence (e.g. Norman & Silk 1983; Poon & Merritt 2004).

Supporting evidence for collisionless loss cone refilling appeared with the first simulations of merging galaxies hosting central MBHs, in which the merger was followed from early times (Preto et al. 2011; Khan et al. 2011; Gualandris & Merritt 2012; Khan et al. 2012) as well as in cosmologically motivated mergers (Khan et al. 2016). In these simulations, the hardening rate of the binary is found to be largely independent of N , and the merger remnant shows significant triaxiality, at least in the central regions. The supply of stars in these cases is sufficiently high to ensure MBH coalescence in much less than a Hubble time. However, the complexity of galaxy merger simulations leaves open the possibility that a different process (that could be physical or a numerical error) is responsible for the sustained binary. If torques from a non-spherical background are responsible for efficient loss cone refilling, the same behaviour should be observed for binaries placed in isolated non-spherical models. The first N -body simulations of BHBs in triaxial galaxy models were performed by Berczik et al. (2006), who considered flattened models with net rotation and $N \leq 10^6$. In this case, an equal mass BHB is found not to stall but to sustain an hardening sufficient to lead to coalescence. On the other hand, Vasiliev et al. (2014) follow the evolution of BHBs in spherical, axisymmetric and triaxial non-rotating isolated models, using direct N -body simulations with particle numbers up to one million. They find an N dependence of the hardening rate in all models, with only a mild flattening at the largest N for the non-spherical models. Hardening rates are higher in non-spherical models than in spherical ones, but always lower than the full loss cone rate. They conclude that collisional effects still contribute significantly to the loss cone repopulation at these N , and prevent a reliable extrapolation to real galaxies. N -body simulations of collisional stellar systems are very expensive, especially when regularisation and/or very small softening are employed to model the evolution of the BHB accurately. A possible solution to limit the effects

of collisional repopulation is to adopt a collisionless numerical method. [Vasiliev et al. \(2015\)](#) follow the evolution of BHBs in isolated models with a Monte Carlo code able to suppress the effects of two-body relaxation. In this case, they find that hardening rates tend to become N -independent in triaxial models in the limit of large N ($N \gtrsim 5 \times 10^6$). Rates are always lower than the full loss cone rate, but in triaxial models they are sufficient to drive BHBs to coalescence in less than a Hubble time. Axisymmetric models, however, have hardening times that are too long to be of interest. This is in contradiction with the results of [Khan et al. \(2013\)](#) for axisymmetric models, and the reason for the discrepancy remains unknown, though likely of numerical origin.

In this study, we present an alternative approach to model the loss cone refilling of BHBs. By means of direct summation simulations of galaxy mergers, we show that a good proxy for the binary hardening rate is given by the integrated number of stars with angular momentum smaller than the loss cone angular momentum of the binary. We estimate this at the hard-binary separation, counting each star only once in the time interval of interest. This is because we expect stars to be scattered out of the loss cone following an interaction. We then consider different isolated galaxy models, spherical and flattened, and follow their evolution with both a direct summation code and a tailored fast multiple method. We show that the hardening rate is a strong function of particle number N in spherical models, with a scaling consistent with expectations for collisional processes. On the other hand, the hardening rate becomes independent of N for $N \gtrsim 5 \times 10^6$, in triaxial models. The behaviour of axisymmetric models is intermediate between that of spherical and triaxial models, with a slow but significant dependence on N . We reach values of N equal of 2 million particles with direct summation and 64 million particles with the fast multiple method. Efficient loss cone refilling is seen even in mildly triaxial models (with axis ratios 1 : 0.9 : 0.8). Such triaxiality is unavoidable following galaxy mergers and drives binaries into the gravitational waves regime. We conclude therefore that there is no ‘final parsec problem’ in the evolution of BHBs even in gas-free systems due to the efficiency of collisionless loss cone refilling in triaxial potentials.

2 THE HARDENING RATE OF BLACK HOLE BINARIES

In this section, we present a semi-analytic model for binary hardening. We will compare this with numerical simulations in section 3. Consider a binary system of two MBHs with masses M_1 and M_2 and semi-major axis a . The total mass of the binary is $M_{\text{bin}} = M_1 + M_2$ and the binding energy is

$$E = \frac{GM_1M_2}{2a} = \frac{G\mu M_{\text{bin}}}{2a} \quad (1)$$

where $\mu = M_1M_2/M_{\text{bin}}$ is the reduced mass. The time-dependent hardening rate of the binary is defined as

$$s \equiv \frac{d}{dt} \left(\frac{1}{a} \right). \quad (2)$$

We define a binary to be ‘‘hard’’ if the binding energy per unit mass exceeds σ^2 , where σ is the stellar velocity

dispersion. The hard binary separation can be defined as

$$a_h = \frac{G\mu}{4\sigma^2} = \frac{M_2}{M_{\text{bin}}} \frac{r_h}{4} \quad (3)$$

where $r_h = GM_1/\sigma^2$ is the influence radius of the most massive MBH. Stars of angular momentum J interact with the binary if $J \leq J_c$, the loss cone angular momentum

$$J_c = \mathcal{K}a\sqrt{2[E - \Phi(\mathcal{K}a)]} \approx \sqrt{2GM_{\text{bin}}\mathcal{K}a}. \quad (4)$$

Here \mathcal{K} is a dimensionless constant of order unity, and in the following we adopt $\mathcal{K} = 1$.

Following the classical analysis by [Hills \(1983\)](#) we define a dimensionless coefficient describing the energy exchange in a single encounter between the binary and a single star of mass m

$$C = \frac{M_{\text{bin}}}{2m} \frac{\Delta E}{E}, \quad (5)$$

where $\Delta E = -(GM_{\text{bin}}/2)\Delta(1/a)$ is the change in binding energy. In the hard binary limit $a \ll a_h$, the outcome of the interaction depends solely on the ratio $\chi = J/J_{\text{bin}}$, where $J_{\text{bin}} = \sqrt{2GM_{\text{bin}}a}$ is the angular momentum of the binary, assumed circular for simplicity.

The change in binary hardness in one encounter is simply:

$$\Delta \left(\frac{1}{a} \right) = \frac{2m}{M_{\text{bin}}a} C(\chi). \quad (6)$$

The hardening rate of a binary in a fixed density background with uniform density ρ and uniform velocity v is the ([Vasiliev et al. 2014](#))

$$s = \frac{\rho v}{m} \int_0^\infty \Delta \left(\frac{1}{a} \right) 2\pi b db = \frac{G\rho}{v} \int_0^\infty 8\pi C(\chi) \chi d\chi. \quad (7)$$

Here we adopt the expression for $C(\chi)$ derived by [Vasiliev et al. \(2014\)](#) for the case of an equal mass circular binary based on the dependence found by [Sesana et al. \(2006\)](#). If we identify

$$H \equiv \int_0^\infty 8\pi C(\chi) \chi d\chi, \quad (8)$$

this is of the form of the expression derived by [Quinlan \(1996\)](#)

$$s_H = \frac{G\rho}{v} H \quad (9)$$

with H a dimensionless hardening coefficient, which reaches an approximately constant value $H_0 \approx 16$ in the hard binary limit $a \ll a_h$. This result implies that a hard binary hardens at a constant rate in a constant density background. Stellar densities do not remain constant during galaxy mergers due to the slingshot ejection of loss-cone stars. A constant or slowly declining hardening rate therefore implies an efficient repopulation of the loss-cone in merger simulations ([Preto et al. 2011](#); [Khan et al. 2011](#); [Gualandris & Merritt 2012](#)).

The hardening rate can be computed in an approximate way directly from the N -body data as the summation of the individual contributions of all stars. In this model, we have

$$s_{NB} = \sum_{i=1}^N \frac{2m_i}{M_{\text{bin}}P_i} \frac{C(\chi)}{a}, \quad (10)$$

where m_i is the mass of the star and P_i its radial orbital

period. In principle, the summation extends to all stars in the system. However, the function $C(\chi)$ quickly falls to zero for $\chi > 1$, with no contribution from stars with $\chi \gtrsim 2$ (Sesana et al. 2006, fig.1).

In the next section, we show that the hardening rates computed from the N -body data are in good agreement with those measured from the binary’s semi-major axis in merger simulations. We also show that restricting the summation in equation 10 to stars with $\chi \leq 1$ still provides a good match while significantly reducing computational cost. We then introduce a proxy for the hardening rate of the binary which depends only on the integrated number of stars with $\chi \leq 1$ over the simulation time and show that, although approximate, this allows us to study loss cone refilling in the collisionless regime.

3 NUMERICAL SIMULATIONS

3.1 Simulations of galaxy mergers

First we perform collisional direct summation N -body simulations of mergers of galaxies harbouring central massive black holes and measure the hardening rate of the black hole binary. For these simulations, we make use of the HiGPUs (Capuzzo-Dolcetta et al. 2013) GPU parallel software. We consider spherical galaxy models following Dehnen’s spherical density profile (Dehnen 1993; Saha 1993)

$$\rho(r) = \frac{(3 - \gamma) M}{4\pi} \frac{a}{a^\gamma (r + a)^{4-\gamma}} \quad (11)$$

where M is the total mass of the galaxy, a the scale radius and γ the asymptotic inner slope. For $\gamma = 1$ equation 11 gives the Hernquist model (Hernquist 1990). We adopt standard N -body units $M = G = a = 1$.

We perform one set of simulations of equal mass galaxies with $\gamma = 1$ and different N from $2^{15} \sim 32k$ to $2^{20} \sim 1$ million. Each model contains a supermassive black hole of mass 0.005, in units of the galaxy mass. The galaxies are placed on a bound elliptical orbit with eccentricity $e = 0.4$ and at an initial distance $D = 5$. The softening length is set to $\epsilon = 10^{-4}$. We follow the evolution of the binary for a time $t_{\text{end}} = 200$. In these units, the formation of a hard binary occurs at $t \sim 50$.

We monitor the evolution of the binary’s semi-major axis a and compute the hardening rate by fitting a straight line to $a^{-1}(t)$ in small time intervals, from the time of binary formation to the end of the integration. The result is shown in Fig. 1 for models with different particle numbers. Naturally, low- N models show considerable noise but we include them for completeness. As the binary shrinks due to gravitational slingshot ejections of interacting stars, the loss cone angular momentum J_{lc} decreases and the hardening rate decreases slowly with time. However, it does so for all considered choices of N , and shows no significant N -dependence. We also consider the hardening rate averaged over a given time-interval: specifically over $50 < t < 100$, $100 < t < 150$ and $150 < t < 200$. The first is meant to capture the phase of quick hardening after the binary becomes formally bound and then reaches the hard-binary separation, while the second and third represent the late phases of hardening, once all the stars initially in the loss cone have been ejected and hardening is due to refilling of the loss cone. The averaged

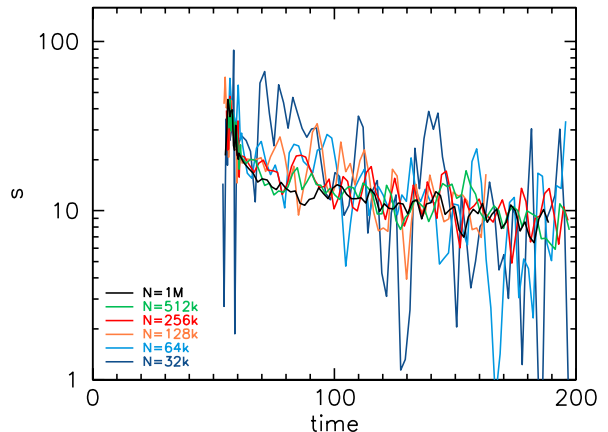


Figure 1. Time dependence of the hardening rate in collisional simulations of galaxy mergers with different particle number N , up to one million.

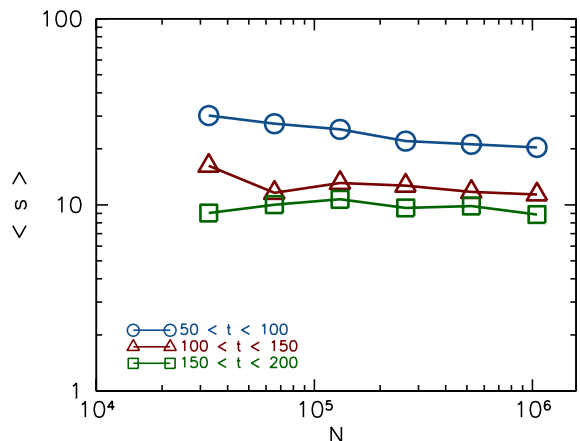


Figure 2. Binary hardening rate in direct collisional simulations of galaxy mergers with different particle number N , averaged over different time intervals: $50 \leq t \leq 100$ (circles), $100 \leq t \leq 150$ (triangles) and $150 \leq t \leq 200$ (squares).

hardening rates are shown in Fig. 2 as a function of particle number. Despite the noise that plagues low- N simulations, there is essentially no dependence of the hardening rate on particle number. This is in agreement with the results of earlier simulations of galaxy mergers (Preto et al. 2011; Khan et al. 2011; Gualandris & Merritt 2012). We find a similar result for a second set of simulations of mergers of equal mass galaxies with a $\gamma = 1.5$ density profile.

We also compute the hardening rate in the merger simulations directly from the N -body data, according to equation 10, both summing up the contributions of all stars and considering only stars with $\chi \leq 1$. For the computation of $C(\chi)$ we adopt the fitting function given in Vasiliev et al. (2014, equation 5) which well approximates the results of Sesana et al. (2006) in the case of a circular, equal mass binary. The radial orbital period of each star is computed by solving numerically the integral

$$P_i = 2 \int_{r_p}^{r_a} \frac{dr}{\sqrt{2[E - \Phi(r)] - J^2/r^2}}, \quad (12)$$

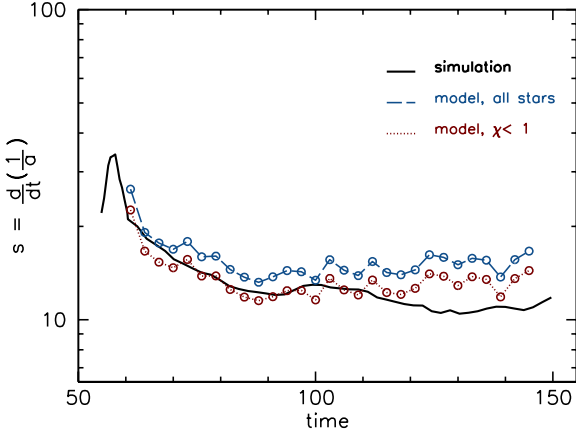


Figure 3. Binary hardening rate versus time measured in a galaxy merger with $N = 10^6$ (solid line) and estimated from the stellar angular momenta according to equation 10 including all stars (dashed line) and only stars with $\chi \leq 1$ (dotted line).

where E and J are, respectively, the energy and angular momentum of the orbit, $\Phi(r)$ is the gravitational potential and the pericentre r_p and apocentre r_a are computed by solving numerically the equation for the turning points in a spherical potential

$$\frac{1}{r^2} + \frac{2[\Phi(r) - E]}{J^2} = 0. \quad (13)$$

The hardening rates computed for the $N = 2^{20} \sim 10^6$ merger simulation are shown in Fig. 3, and compared with the rate measured from the binary’s semi-major axis according to the definition given in equation 2. The agreement is quite good, also in the case when the contribution from stars with $\chi > 1$ is neglected.

We now look for a simple proxy for the binary hardening rate that depends only on the angular momenta of the stars. Given that, at any time, the hardening of the binary is due to stars with angular momentum smaller than the loss cone angular momentum $J \leq J_{lc}$, we consider as proxy for the hardening rate the parameter

$$\mathcal{R}_J \equiv \frac{N_J}{N} = \frac{N(J \leq J_{lc})}{N} \quad (14)$$

where N_J is the total number of stars with initial angular momentum larger than the loss cone angular momentum at the hard binary separation $J > J_{lc}(a_h)$ but which reach $J < J_{lc}$ at some point in the simulation. In particular, stars moving in and out of the loss-cone are counted only once, to account for the fact that they would be ejected after a close encounter with the BHB. We will refer to \mathcal{R}_J as the refilling parameter.

We compute the loss cone refilling parameter in the merger simulations, where we assumed three different values for the loss cone angular momentum, representative of binaries with different total mass in units of the galaxy mass. The results, shown in Fig. 4, indicate that while N_J is a strong function of N for all considered values of J_{lc} (see top panel), the refilling parameter \mathcal{R}_J is effectively independent of N (see bottom panel). The refilling parameter is therefore a reliable proxy for the binary hardening rate: if \mathcal{R}_J is independent of N , so is the hardening rate.

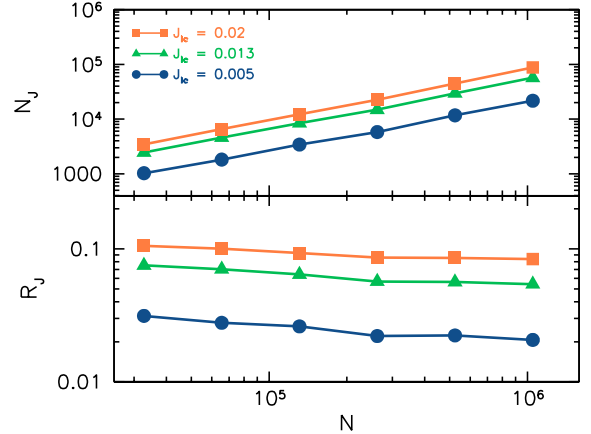


Figure 4. Top: total number of stars with angular momentum $J \leq J_{lc}$, representative of the loss cone angular momentum at the hard binary separation for binaries with different total mass. N_J was computed in the merger simulations with initial $\gamma = 1.0$ profile. Each star satisfying the condition is counted only once and stars satisfying the condition at the start of the simulations are discounted. Bottom: refilling parameter, as defined in equation 14, in the merger simulations.

3.2 Simulations of isolated models

The refilling parameter depends only on the number of stars with angular momentum smaller than a given critical value, i.e. only on the fraction of stars able to interact with the binary during the hardening phase. This, in turn, depends on the level of non-sphericity of the gravitational potential. Therefore, it is not necessary to perform simulations of galaxy mergers with massive black holes in order to model collisionless loss cone refilling. Such simulations are required for a precise determination of the hardening rate and the coalescence timescale, but not to ascertain the fate of BHBs in the broader context of the final parsec problem. Simulations including BHBs are computationally very expensive because of two main reasons: (i) direct summation is usually implemented for the computation of gravitational forces (ii) a small gravitational softening is adopted to follow the evolution of the binary to very small separations, well below the hard-binary limit.

Here we take a different approach in which we simulate isolated galaxy models without massive black holes and estimate the collisionless loss cone refilling rate by measuring the refilling parameter in models with increasing N . We adopt both a direct summation technique, with particle numbers up to $2^{21} \sim 2$ millions, and a tailored fast multiple method, with particle numbers up to $2^{26} \sim 64$ million. For the former set of simulations we use the ϕ GRAPE code (Harfst et al. 2007), adapted to run on a GPU cluster by means of the SAPPORO library (Gaburov et al. 2009). For the latter set of simulations we adopt the collisionless N -body code GRIFFIN, which employs the fast multipole method (FMM). To allow for softened gravity, the FMM is implemented in Cartesian coordinates, but otherwise is very similar to the method reported in (Dehnen 2014), in particular the computational effort at a given accuracy is minimised while maintaining a well behaved distribution of errors. In this way, the code can be made as accurate as direct sum-

Model	Axis ratios	M_{bin}/M	r_m	a_h	J_{LC}
S	1:1:1	0.001	0.13	0.008	0.004
S	1:1:1	0.005	0.22	0.014	0.012
S	1:1:1	0.01	0.28	0.018	0.018
A	1:1:0.8	0.001	0.13	0.008	0.004
A	1:1:0.8	0.005	0.22	0.014	0.012
A	1:1:0.8	0.01	0.28	0.017	0.019
T1	1:0.9:0.8	0.001	0.25	0.015	0.0055
T1	1:0.9:0.8	0.005	0.41	0.025	0.016
T1	1:0.9:0.8	0.01	0.50	0.032	0.025
T2	1:0.8:0.6	0.001	0.26	0.016	0.0057
T2	1:0.8:0.6	0.005	0.44	0.027	0.016
T2	1:0.8:0.6	0.01	0.55	0.034	0.026

Table 1. Parameters used to estimate the loss cone angular momentum in spherical (S), axisymmetric (A) and triaxial (T) models. The columns indicate, respectively, the model name, the axis ratio, the mass of the hypothetical black hole binary in units of the total galaxy mass, the influence radius of the black hole binary, the hard-binary separation and the resulting loss cone angular momentum.

mation with a $\mathcal{O}(N)$ scaling. The simulations reported here use multipole expansion order $p = 5$ and a relative force error of 5×10^{-5} for each particle. Initially, we attempted to use the public N -body code GADGET2, but could not obtain converged results (see Appendix A), most likely owing to insufficient force accuracy of the tree method.

Very large particle numbers are required to eliminate collisional effects and measure collisionless repopulation of the loss cone, as these occur on a relaxation time scale, which scales as $N/\ln N$. However, we also perform direct summation simulations to validate the results of the fast multiple method code and to compare with existing results.

We consider galaxy models following a generalisation of the Hernquist (1990) profile

$$\rho(r) = \frac{M}{2\pi abc} \frac{1}{r(1+r)^3} \quad (15)$$

to allow for non-sphericity, where a, b, c represent the axes of a triaxial ellipsoid. Units are such that $M = 1$, where M is the total mass of the galaxy, and $abc = 1$.

The parameters of all the models are listed in Table 1, including spherical models, axisymmetric models with axis ratios 1:1:0.8 and two sets of triaxial models, moderately triaxial with 1:0.9:0.8 and triaxial with 1:0.8:0.6.

All models were generated with the SMILE software (Vasiliev 2013), a recent implementation of the Schwarzschild orbital superposition method, using 2×10^5 orbits.

We adopt an N dependent value of softening appropriate for the FMM code of the order

$$\epsilon \approx \left(\frac{2\pi}{N}\right)^{\frac{1}{3}} \quad (16)$$

and apply the same to the ϕ GRAPE simulations. While this choice is larger than the values generally employed in direct summation simulations, it is appropriate for the collisionless process to be studied here. A more detailed description of the effect of softening is given in section 3.3.

Figure 5 shows the refilling parameter \mathcal{R}_J as a function of particle number for all the models and with both codes, assuming a loss cone angular momentum $J_{\text{lc}} = 0.005$ and $J_{\text{lc}} = 0.02$. These values correspond to the cases of binary to galaxy mass ratio of 0.001 and 0.01, respectively (see Table 1). We find that for spherical models \mathcal{R}_J decreases with N as $1/\sqrt{N}$, a signature that in these models collisional effects are responsible for loss cone refilling. This holds true even at the largest N reached with GRIFFIN. In triaxial models, instead, the behaviour is dramatically different. Not only is \mathcal{R}_J much larger in the triaxial models than in the spherical ones, there is essentially little or no N dependence, as expected if a collisionless process is responsible for refilling the loss cone. The systematically larger values of \mathcal{R}_J in the more triaxial models (T2) compared to the moderately triaxial ones (T1) also supports the interpretation that the shape of the potential is the key element in the refilling process. Axisymmetric models show a behaviour which is intermediate between that of the spherical and triaxial models, with a refilling parameter which decreases as a function of N as in spherical models, but much more slowly. This can be interpreted as a consequence of the nature of orbits in an axisymmetric potential, where the total angular momentum J of individual particles is not conserved but J_z is, and there is therefore a lower limit to how small J can become during the evolution. In the case of the largest J_{lc} , there is evidence for flattening at the largest N , but convergence is certainly not yet reached in these models. The implication for BHBs in merger remnants is therefore that flattening of the system may not be sufficient to sustain orbital decay to the gravitational wave phase, but that a certain, even moderate, degree of triaxiality may be needed to drive the binaries to coalescence within a Hubble time. This is in good agreement with the findings of Vasiliev et al. (2015). Figure 6 shows the refilling parameter computed for just the J_z component of stellar angular momentum. Because this component is conserved for stars in an axisymmetric potential, \mathcal{R}_{J_z} shows the same N dependence in axisymmetric models as in spherical models. On the other hand, there is no N dependence in triaxial models, as expected.

Our computation of the refilling parameter as a proxy for the hardening rate relies on the assumption that stars whose angular momentum falls below the binary angular momentum populate the loss cone and will eventually interact with the binary, contributing to its orbital decay. In order to verify this assumption we compute the number of stars within a given distance from the centre of the system and look for correlations between this quantity and N_J . In particular, we define N_r as the number of stars initially within a distance $r > r_h$ equal to the the hard binary separation which obtain $r < r_h$ at some time during the simulation. For our fiducial choice of mass ratios $M_{\text{bin}}/M = 0.001, 0.005, 0.01$ this corresponds to $r_h = 0.008, 0.014, 0.018$.

We find that N_r correlates with N_J in all models, both spherical and non-spherical, as shown in figure 7. We also find the expected difference between spherical and triaxial models, with the latter showing much larger values of N_r than the corresponding spherical models with the same N . The same holds for models T1 and T2, where the more triaxial set systematically has larger values of N_r . As usual,

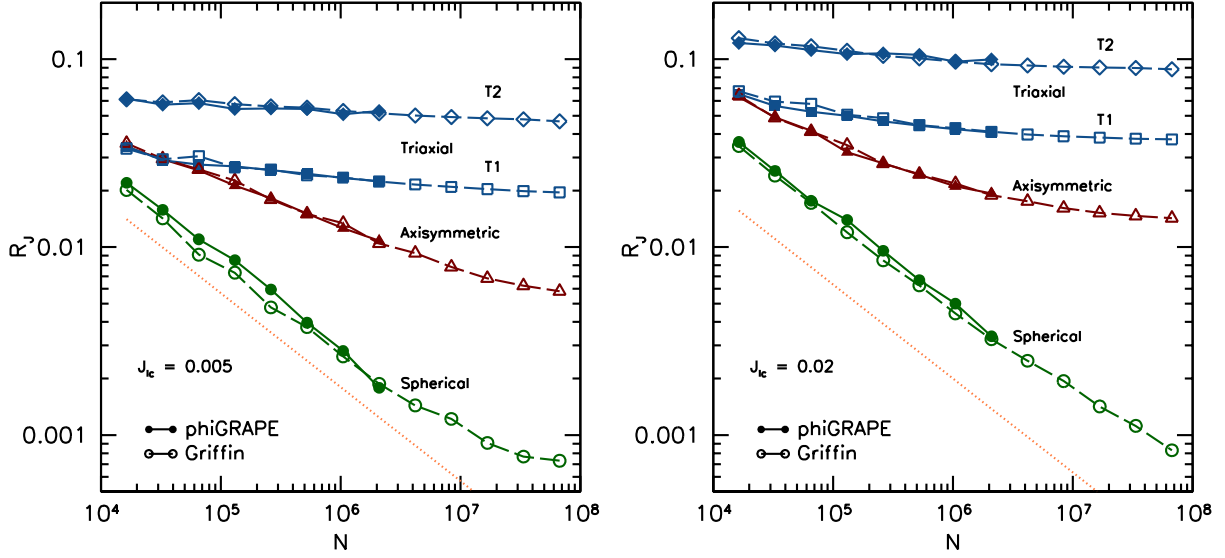


Figure 5. Refilling parameter \mathcal{R}_J as a function of particle number for different models assuming a loss cone angular momentum $J_{lc} = 0.005$ (left) and $J_{lc} = 0.02$ (right). In both panels the dotted line shows the $1/\sqrt{N}$ slope expected for collisional loss cone repopulation.

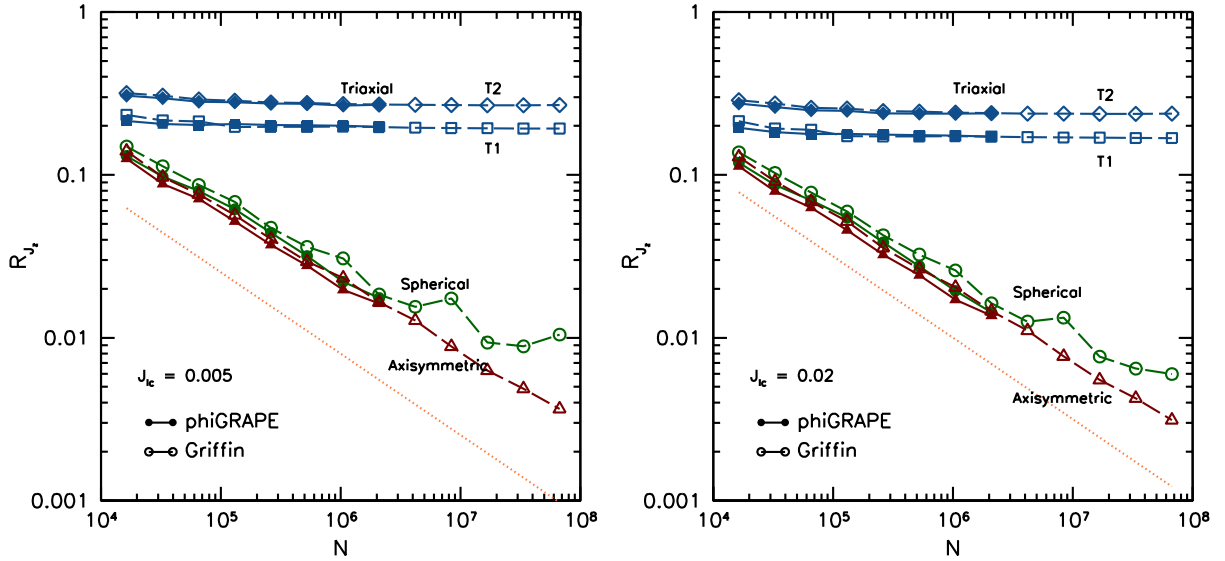


Figure 6. Refilling parameter \mathcal{R}_{J_z} as a function of particle number for different models assuming a loss cone angular momentum $J_{lc} = 0.005$ (left) and $J_{lc} = 0.02$ (right). In both panels the dotted line shows the $1/\sqrt{N}$ slope expected for collisional loss cone repopulation.

axisymmetric model lie in between the spherical and the triaxial models.

To determine the final fate of BHBs, we also computed the numerical hardening rate s_{NB} as given in equation 10, assuming a starting value of the binary semi-major axis equal to the one measured in the merger simulation with $\gamma = 1$ and $N = 10^6$. In order to mimic the erosion of the stellar cusp produced by a BHB, we assume that stars are lost after a time equal to their radial orbital period and

therefore do not contribute to the hardening rate at later times. The rates for spherical and non-spherical models with $N = 10^6$ are shown in Fig. 8 as a function of time. We find that the triaxial models well reproduce the time evolution of the hardening rates measured in the merger simulation, while the spherical model shows an hardening rate that is more than one order of magnitudes lower. The axisymmetric model is intermediate, with rates significantly lower than the merger simulation. The rates for the merger simulation lie in

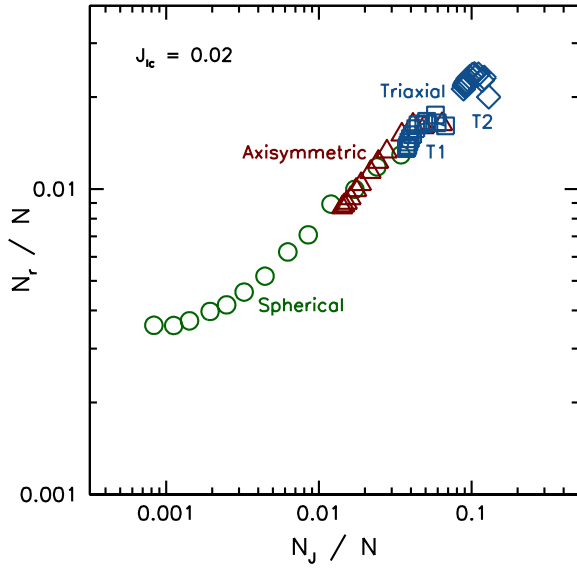


Figure 7. Correlation between the number of stars N_r within a given distance from the centre and the number of stars N_J with angular momentum smaller than the loss cone angular momentum, for spherical (circles), axisymmetric (triangles) and triaxial (diamonds) models. All models were evolved with GRIFFIN and the refilling parameter is computed with $J_{lc} = 0.02$, while N_r is computed for a distance $r_{lc} = 0.018$ from the centre, corresponding to the hard binary separation of a black hole binary with mass of 1% of the galaxy mass.

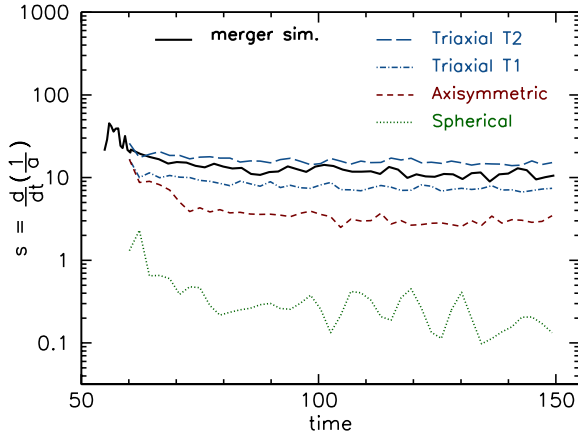


Figure 8. Hardening rate in the spherical (dotted line), axisymmetric (short dashed line) and triaxial (dot-dashed and long dashed lines) isolated models as a function of time. For a comparison, the hardening rate measured in the merger simulation with $\gamma = 1$ and $N = 10^6$ is also shown (thick solid line).

between those of model T2, with axis ratios 1 : 0.8 : 0.6 and model T1, with axis ratios 1 : 0.9 : 0.8. At the time of binary formation, the merger remnant can be best fit by a triaxial ellipsoid with axis ratios 1 : 0.8 : 0.6 at a distance $D = 0.5$ from the binary's centre of mass, and by a triaxial ellipsoid with axis ratios 1 : 0.9 : 0.7 at a distance $D = 1$. The shape of the remnant is therefore consistent with an isolated model

of triaxiality that is intermediate between that of models T1 and T2. On the other hand, one might expect the hardening of the merger remnant to be enhanced compared to that of an isolated model due to rotation, which has been shown to lead to higher hardening rates (Holley-Bockelmann & Khan 2015). The small discrepancy might be due to the fact that the simple semi-analytic approach used to compute s_{NB} assumes that any star with $\chi < 1$ will interact with the binary within an orbital period, and this might not always be the case.

The hardening rate may also be artificially increased by Brownian motion, a wandering of the binary which leads to an enlarged loss-cone (Merritt 2001; Chatterjee et al. 2003). Using dedicated N -body simulations, however, Bortolas et al. (2016) find that Brownian motion does not affect the evolution of BHBs in simulations with N in excess of one million.

The timescale for coalescence from a separation a due to emission of gravitational waves is, for a circular binary,

$$T_{\text{GW}} = \frac{5}{256} \frac{c^5 a^4}{G^3 M_1 M_2 M_{\text{bin}}} \approx 5.8 \times 10^8 \text{ yr} \left(\frac{a}{10^{-3} \text{ pc}} \right)^4 \left(\frac{10^6 M_{\odot}}{M_{\text{bin}}} \right)^3. \quad (17)$$

Therefore, for a given binary mass the separation corresponding to a time shorter than a Hubble time is

$$a_{\text{GW}} \approx 2 \times 10^{-3} \text{ pc} \left(\frac{M_{\text{bin}}}{10^6 M_{\odot}} \right)^{3/4}. \quad (18)$$

This corresponds to approximately $a_{\text{GW}} \sim 0.01 a_h$ for all considered models. The total time to coalescence is given by the time spent in hardening down to a separation of the order of a_{GW} plus the time T_{GW} for inspiral. For the models considered above for the computation of s_{NB} with $M_{\text{bin}} = 10^6 M_{\odot}$ and extrapolating the evolution of $a(t)$ to later times, we find that both the triaxial and axisymmetric models would be able to reach coalescence within a Hubble time. However, for typical systems with $M_{\text{bin}} \sim 10^8 M_{\odot}$ only the triaxial models have hardening rates large enough to ensure coalescence. The rates for the axisymmetric models are too low to bridge the gap to the gravitational waves dominated regime. These results are in good agreement with those of Vasiliev et al. (2015).

3.3 Effect of numerical softening

The refilling parameter measured in the isolated models depends on the numerical softening chosen in the simulations. Softening reduces the collisionality of a stellar system by suppressing the importance and the effect of close encounters. Therefore it is natural to expect a dependence of the refilling parameter on softening in spherical systems, in which loss cone refilling is dominated by collisional effects. In triaxial models, collisional and collisionless modes of losscone repopulation coexist at the modest particle numbers typical of direct summation simulations. If a small softening is used, as in the simulations of Vasiliev et al. (2014) including the BHB, very large particle numbers are required for collisionless refilling to become dominant. Hence their conclusion that much larger N values than affordable by direct summation are necessary to suppress relaxation effects. On

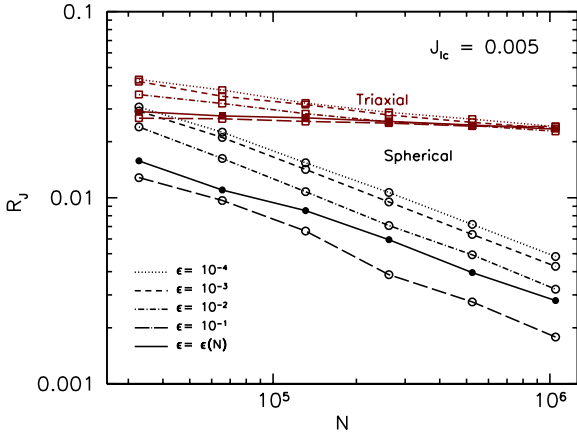


Figure 9. Refilling parameter as a function of particle number in direct summation integrations of spherical (circles) and triaxial (squares) models with different values of softening. Empty symbols refer to fixed values of softening for all particle numbers, while filled symbols refer to the N -dependent prescription defined in equation 16.

the other hand, adopting a larger value of softening, as done in this work for models without MBHs, allows the effects of global torques to become apparent at smaller particle numbers.

Figure 9 shows the dependence of R_J on softening in ϕ GRAPE integrations of spherical and triaxial models. We consider cases in which a fixed softening is adopted for models of different N (empty symbols) and the case of N -dependent softening defined in equation 16 (filled symbols). In the spherical models R_J decreases with increasing softening as expected, and the choice of the variable softening works well at reducing collisional effects. In triaxial models the effect of a larger softening is to reduce scatterings into the loss cone and the flattening of R_J appears at smaller N .

4 DISCUSSION AND CONCLUSIONS

Black hole binary hardening in simulations of galaxy mergers is believed to be sustained by a collisionless mode of loss cone refilling which owes to global torques in non-spherical potentials. This is necessary to ensure hardening down to separations where emission of gravitational waves becomes dominant and leads the black holes to coalescence. Merger remnants typically show a significant degree of flattening and a modest departure from axisymmetry (Preto et al. 2011; Khan et al. 2011; Gualandris & Merritt 2012), which argues for a significant population of stars on centrophilic orbits. However, if this is indeed the case then binary hardening should also be efficient in isolated triaxial models. Simulations by Vasiliev et al. (2014) show that collisionless losscone refilling is masked by collisional refilling due to stellar scatterings in simulations with modest particle numbers and small softening. Here we take a different approach to the problem and study losscone refilling in isolated galaxy models. In order to reduce the effects of collisionality we perform simulations with the fast multiple method code GRIFFIN (Dehnen 2014), which allows us to increase particle number to 64 million. We find a proxy for binary hardening,

which is given by the refilling parameter, i.e. the fraction of stars with angular momentum smaller than the angular momentum of an hypothetical BHB of given mass, where each star is counted only once per simulation.

Our key findings are:

- The refilling parameter, i.e. the fraction of stars which can be counted at least once to have angular momentum smaller than the loss cone angular momentum, is a good proxy for the hardening rate in merger simulations.
- Loss cone refilling in spherical models depends critically on particle number, a clear signature that it is driven by two body scatterings. In real galaxies, this process becomes extremely inefficient and BHBs are not expected to reach the gravitational wave phase.
- There is no N -dependence of the refilling parameter in triaxial models above $N \sim 10^7$. Refilling is more efficient in triaxial models than in spherical models, and a higher degree of triaxiality also leads to more efficient refilling.
- Axisymmetric models have properties in between spherical and triaxial models. While refilling is consistently more efficient than in spherical cases, we observe a marked N -dependence with no obvious flattening even at the largest N values.
- Hardening rates computed directly from the N -body data in isolated triaxial models match those computed in merger simulations. On the other hand, spherical isolated models and axisymmetric models have significantly lower hardening rates.
- The hardening rates measured for the triaxial models are large enough to ensure coalescence of the binaries within a Hubble time for Milky Way type galaxies as well as more massive ones. Hardening rates in axisymmetric models are only marginally sufficient to bridge the gap to the gravitational waves regime in the case of low mass binaries ($M_{\text{bin}} \lesssim 10^6 M_{\odot}$) but imply coalescence times that are longer than a Hubble time for typical binaries ($M_{\text{bin}} \sim 10^8 M_{\odot}$). Spherical models are generally characterised by hardening rates too low to lead to coalescence.

ACKNOWLEDGMENTS

This work used the GPU cluster of the Astrophysics group, University of Surrey, and the DiRAC Complexity system, operated by the University of Leicester IT Services, which forms part of the STFC DiRAC HPC Facility (www.dirac.ac.uk). This equipment is funded by BIS National E-Infrastructure capital grant ST/K000373/1 and STFC DiRAC Operations grant ST/K0003259/1. DiRAC is part of the National E-Infrastructure. We thank Eugene Vasiliev for support with the SMILE software and Andrew Pontzen for interesting discussions.

REFERENCES

- Abbott B. P. et al., 2016a, Phys. Rev. Lett., 116, 061102
 Abbott B. P. et al., 2016b, Phys. Rev. Lett., 116, 241103
 Babak S. et al., 2016, MNRAS, 455, 1665
 Barausse E., Bellovary J., Berti E., Holley-Bockelmann K., Farris B., Sathyaprakash B., Sesana A., 2015, Journal of Physics Conference Series, 610, 012001

- Begelman M. C., Blandford R. D., Rees M. J., 1980, *Nature*, 287, 307
- Berczik P., Merritt D., Spurzem R., 2005, *ApJ*, 633, 680
- Berczik P., Merritt D., Spurzem R., Bischof H.-P., 2006, *ApJL*, 642, L21
- Bortolas E., Gualandris A., Dotti M., Spera M., Mapelli M., 2016, *MNRAS*, 461, 1023
- Capuzzo-Dolcetta R., Spera M., Punzo D., 2013, *Journal of Computational Physics*, 236, 580
- Chatterjee P., Hernquist L., Loeb A., 2003, *ApJ*, 592, 32
- Cuadra J., Armitage P. J., Alexander R. D., Begelman M. C., 2009, *MNRAS*, 393, 1423
- Dehnen W., 1993, *MNRAS*, 265, 250
- Dehnen W., 2014, *Computational Astrophysics and Cosmology*, 1, 1
- Dotti M., Sesana A., Decarli R., 2012, *Advances in Astronomy*, 2012, 3
- Faber S. M. et al., 1997, *AJ*, 114, 1771
- Ferrarese L. et al., 2006, *ApJS*, 164, 334
- Gaburov E., Harfst S., Portegies Zwart S., 2009, *New A*, 14, 630
- Graham A. W., 2004, *ApJL*, 613, L33
- Graham A. W., 2013, *Elliptical and Disk Galaxy Structure and Modern Scaling Laws*, Oswalt T. D., Keel W. C., eds., p. 91
- Gualandris A., Merritt D., 2012, *ApJ*, 744, 74
- Harfst S., Gualandris A., Merritt D., Spurzem R., Portegies Zwart S., Berczik P., 2007, *New Astronomy*, 12, 357
- Hernquist L., 1990, *ApJ*, 356, 359
- Hills J. G., 1983, *AJ*, 88, 1269
- Hogan C. J., Schutz B. F., Cutler C. J., Hughes S. A., Holz D. E., 2009, in *Astronomy*, Vol. 2010, *astro2010: The Astronomy and Astrophysics Decadal Survey*
- Holley-Bockelmann K., Khan F. M., 2015, *ApJ*, 810, 139
- Khan F. M., Berentzen I., Berczik P., Just A., Mayer L., Nitadori K., Callegari S., 2012, *ApJ*, 756, 30
- Khan F. M., Fiacconi D., Mayer L., Berczik P., Just A., 2016, *ArXiv e-prints*
- Khan F. M., Holley-Bockelmann K., Berczik P., Just A., 2013, *ApJ*, 773, 100
- Khan F. M., Just A., Merritt D., 2011, *ApJ*, 732, 89
- Lauer T. R., 1985, *ApJ*, 292, 104
- Lauer T. R. et al., 1995, *AJ*, 110, 2622
- Lauer T. R. et al., 2005, *AJ*, 129, 2138
- Lodato G., Nayakshin S., King A. R., Pringle J. E., 2009, *MNRAS*, 398, 1392
- Makino J., Funato Y., 2004, *ApJ*, 602, 93
- Merritt D., 2001, *ApJ*, 556, 245
- Merritt D., 2013, *Dynamics and Evolution of Galactic Nuclei*
- Merritt D., Mikkola S., Szell A., 2007, *ApJ*, 671, 53
- Merritt D., Vasiliev E., 2011, *ApJ*, 726, 61
- Milosavljević M., Merritt D., 2001, *ApJ*, 563, 34
- Milosavljević M., Merritt D., 2003, *ApJ*, 596, 860
- Norman C., Silk J., 1983, *ApJ*, 266, 502
- Pontzen A., Read J. I., Teyssier R., Governato F., Gualandris A., Roth N., Devriendt J., 2015, *MNRAS*, 451, 1366
- Poon M. Y., Merritt D., 2004, *ApJ*, 606, 774
- Preto M., Berentzen I., Berczik P., Spurzem R., 2011, *ApJL*, 732, L26+
- Quinlan G. D., 1996, *New A*, 1, 35
- Quinlan G. D., Hernquist L., 1997, *New A*, 2, 533
- Saha P., 1993, *MNRAS*, 262, 1062
- Sesana A., Haardt F., Madau P., 2006, *ApJ*, 651, 392
- Vasiliev E., 2013, *MNRAS*, 434, 3174
- Vasiliev E., Antonini F., Merritt D., 2014, *ApJ*, 785, 163
- Vasiliev E., Antonini F., Merritt D., 2015, *ApJ*, 810, 49

APPENDIX A: ON THE IMPORTANCE OF FORCE ERRORS

Moving from a direct summation force calculation to a faster approximate method may seem a like natural step when trying to increase particle number in order to reduce collisional effects. However, we caution the reader that care needs to be taken when choosing an approximate method for this type of problem. In order to study diffusion in angular momentum driven by global torques, the force errors need to be sufficiently small. Dehnen (2014) presents an analysis of the force errors for the fast multiple method (or tree code) with a conventional geometric multipole-acceptance criterion (based on an opening angle θ). When using sufficiently large expansion order p and small θ , the relative force errors of such a method can be reduced to 10^{-7} , the same level as contemporary implementations of direct summation. However, the approximated methods show extended tails towards large force errors, a direct consequence of the simple geometric opening criterion. This tail of a few stars with large force errors does not compromise global energy conservation but may seriously affect the validity of simulations, in particular if accurate representation of orbits is required. Our method of choice, GRIFFIN, uses another type of opening criterion, which is informed by an error estimate based on the multipole moments themselves (see Dehnen 2014, for details), and produces a well-behaved distribution of force errors while minimising the computational costs to obtaining a scaling better than $\mathcal{O}(N)$.

Fig. A1 shows a comparison between GADGET2 (a conventional tree code with geometric opening criterion), ϕ GRAPE and GRIFFIN for the calculation of the refilling parameter in spherical and triaxial models of varying N (using the same N -dependent softening for all codes). Values of \mathcal{R}_J agree remarkably well between ϕ GRAPE and GRIFFIN. For a collision-dominated scenario (spherical), GRIFFIN errs slightly towards too small \mathcal{R}_J , which can be understood by a less accurate time integration of two-body encounters, resulting in less scattering. For the collisionless scenario (triaxial), GRIFFIN agrees very well with ϕ GRAPE, despite relative force errors which are ~ 500 times less accurate ($\times 10^{-7}$ vs. 5×10^{-5}). The results from GADGET2 are markedly different and do not reproduce the expected scaling with increasing N , but give too large \mathcal{R}_J with considerable scatter. This erroneous behaviour is exactly what one expects from a few large force errors, which act like a random relaxation process.

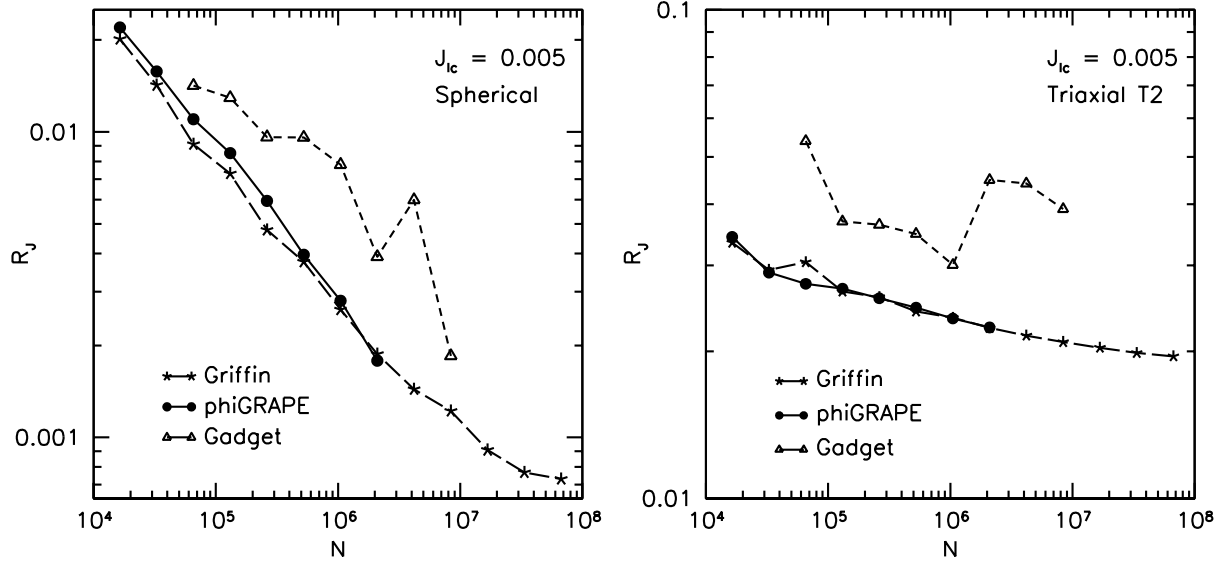


Figure A1. Repopulation parameter versus particle number in spherical (left) and triaxial (right) models, evolved with three different codes: GADGET2 (triangles), ϕ GRAPE (circles) and GRIFFIN (stars).